Unclassified

SECURITY CLASSIFICATION OF THIS PAGE

REPORT DOCUMENTATION PAGE

Form Approved OMB No. 0704-0188

1a. REPORT SECURITY CLASSIFICATION: Unclassified	1b. RESTRICTIVE MARKINGS
2a. SECURITY CLASSIFICATION AUTHORITY	3. DISTRIBUTION/AVAILABILITY OF REPORT: Approved for public release; Distribution unlimited.
2b. DECLASSIFICATION/DOWNGRADING SCHEDULE	
4. PERFORMING ORGANIZATION REPORT NUMBER(S): GL-TR-90-0046	5. MONITORING ORGANIZATION REPORT NUMBER(S)
6a. NAME OF PERFORMING ORGANIZATION: Geophysics Laboratory; 6b. OFFICE SYMBOL (If applicable): PHK	7a. NAME OF MONITORING ORGANIZATION
6c. ADDRESS (City, State, and ZIP Code): Hanscom AFB, Massachusetts 01731-5000	7b. ADDRESS (City, State, and ZIP Code)
8a. NAME OF FUNDING/SPONSORING ORGANIZATION; 8b. OFFICE SYMBOL (If applicable)	9. PROCUREMENT INSTRUMENT IDENTIFICATION NUMBER
8c. ADDRESS (City, State, and ZIP Code)	10. SOURCE OF FUNDING NUMBERS

PROGRAM ELEMENT NO	PROJECT NO	TASK NO	WORK UNIT ACCESSION NO
61102F	2303	G2	01

11. TITLE (Include Security Classification)
Cross Section and Product Time-of-Flight Measurements of the Reaction of N_2^+ With H_2O and D_2O at Suprathermal Energies

12. PERSONAL AUTHOR(S)
Rainer A. Dressler, James A. Gardner*, Richard H. Salter, Francis J. Wodarczyk#, Edmond Murad

13a. TYPE OF REPORT	13b. TIME COVERED	14. DATE OF REPORT (Year, Month, Day)	15. PAGE COUNT
Reprint	FROM _____ TO _____	1990 March 7	9

16. SUPPLEMENTARY NOTATION
*Geophysics Research Scholar #Air Force Office of Scientific Research, Bolling AFB, Washington, D.C. 20332
Reprinted from J. Chem. Phys. 92(2) 15 January 1990

17. COSATI CODES		
FIELD	GROUP	SUB-GROUP

18. SUBJECT TERMS (Continue on reverse if necessary and identify by block number)
Ion-Neutral, Collisions, H_2O^+, N_2^+, H_2O, [illegible]

19. ABSTRACT (Continue on reverse if necessary and identify by block number)

Charge exchange and hydrogen atom pickup cross sections, and product ion time-of-flight measurements are reported for N_2^+–$H_2O(D_2O)$ collisions at center-of-mass collision energies ranging between 1 and 15 eV. No isotope effect is detected for the charge exchange branch, while a significant isotope effect is observed for the atom pickup reaction. Throughout the measured energy range, the time-of-flight measurements show that the $H_2O^+(D_2O^+)$ charge exchange product is produced with near-thermal energy in the laboratory frame, implying little or no momentum transfer. The charge exchange reaction products are therefore formed with internal energy comparable to the exothermicity of the reaction (2.96 eV). The atom pickup ion product velocity distributions and the atom pickup isotope effect are consistent with a spectator stripping mechanism.

20. DISTRIBUTION/AVAILABILITY OF ABSTRACT	21. ABSTRACT SECURITY CLASSIFICATION
☐ UNCLASSIFIED/UNLIMITED ☒ SAME AS RPT. ☐ DTIC USERS	Unclassified

22a. NAME OF RESPONSIBLE INDIVIDUAL	22b. TELEPHONE (Include Area Code)	22c. OFFICE SYMBOL
E. Murad	(617) 377-3176	PHK

DD Form 1473, JUN 86 — Previous editions are obsolete. — SECURITY CLASSIFICATION OF THIS PAGE: Unclassified

Cross section and product time-of-flight measurements of the reaction of N_2^+ with H_2O and D_2O at suprathermal energies

Rainer A. Dressler, James A. Gardner,[a] Richard H. Salter, Francis J. Wodarczyk,[b] and Edmond Murad

Geophysics Laboratory, GL/PHK, Hanscom Air Force Base, Massachusetts 01731

(Received 7 August 1989; accepted 5 October 1989)

Charge exchange and hydrogen atom pickup cross sections, and product ion time-of-flight measurements are reported for $N_2^+ - H_2O(D_2O)$ collisions at center-of-mass collision energies ranging between 1 and 15 eV. No isotope effect is detected for the charge exchange branch, while a significant isotope effect is observed for the atom pickup reaction. Throughout the measured energy range, the time-of-flight measurements show that the H_2O^+ (D_2O^+) charge exchange product is produced with near-thermal energy in the laboratory frame, implying little or no momentum transfer. The charge exchange reaction products are therefore formed with internal energy comparable to the exothermicity of the reaction (2.96 eV). The atom pickup ion product velocity distributions and the atom pickup isotope effect are consistent with a spectator stripping mechanism.

I. INTRODUCTION

Ion–molecule reactions have been studied in great detail at energies below 1 eV. At low energies the long-range ion-induced dipole interaction may lead to the formation of a long-lived collision complex, which is expected to dissociate statistically into the energetically possible reactant and product states. Phase space theory[1–3] has frequently been used to reproduce the respective reaction rates determined with low energy techniques such as the flowing afterglow,[4] ICR instrumentation,[4] and the guided ion beam experiment.[5]

At collision energies above 1 eV, the intermediate collision complex usually becomes too short-lived for the successful use of statistical theories, and nonadiabatic processes become more important. Research at these collision energies has been less extensive. Most of the experiments have consisted in determining the energy dependence of the ion–molecule reaction cross section. Crossed beam experiments[4] have yielded important information on the reaction dynamics through the analysis of the kinetic energy and the angular distributions of the product ions.

Recent space measurements of the plasma surrounding the space shuttle have revealed ionization levels greater than ambient densities.[6,7] These measurements have renewed the interest in ion-neutral chemistry at suprathermal relative velocities comparable with the shuttle orbital velocity of 7.7 ± 0.2 km s^{-1}. It is at these relative velocities that ambient ions collide with the contaminant cloud surrounding a spacecraft. The ionized atmosphere in low earth orbit (altitude 200–400 km) consists primarily of O^+ ($\sim$99%) and N_2^+ ($\sim$1%) at a total ion density of about 2×10^5 cm^{-3}.[8] Mass spectrometric measurements show that the local environment of the space shuttle contains relatively large densities of H_2O^+ and H_3O^+.[6,7] These ions undoubtedly originate through charge transfer between ambient ions and H_2O.[9–12] Sources of water vapor include surface outgassing, firing of attitude control jets, and water releases.

Attempts at developing models[9–13] which predict the nature of the space shuttle local environment require a knowledge of the relevant rate coefficients as a function of energy. An understanding of the energy partitioning in the reaction products is also necessary to determine the collision and internal energies at which secondary reactions occur, and to interpret the results from space-borne mass spectrometers whose detection efficiency depends on the ion kinetic energy. The energy dependence of the charge exchange reaction

$$O^+ + H_2O \rightarrow O + H_2O^+ \qquad (1)$$

has been measured previously.[14,15] In order to develop a quantitative code, however, it is necessary to include all reactions of H_2O.

In this paper we report a dynamic study of reactive $N_2^+ - H_2O(D_2O)$ collisions at center-of-mass collision energies ranging between 1 and 15 eV. Two channels are known:

$$N_2^+ + H_2O(D_2O) \rightarrow N_2 + H_2O^+(D_2O^+) \qquad (2a)$$

$$\rightarrow N_2H^+(N_2D^+) + OH(OD). \qquad (2b)$$

A thermal rate constant for reaction (2a) of $(2.19 \pm 0.30)\times10^{-9}$ cm^3 s^{-1} was obtained by Howard *et al.*[16] using the flowing afterglow technique. Turner and Rutherford[17] measured the energy dependence of the cross section for reactions (1) and (2a) and other charge transfer reactions with H_2O in a crossed beam apparatus. These authors measured cross sections for reaction (2a) that are significantly higher than those obtained for reaction (1). Their data for reaction (1), which exhibits an increase in the integral cross section as the primary ion energy increases from 1 to 10 eV, is in poor agreement with measurements of Heninger *et al.*,[15] who observed a declining cross section in the same energy range using a triple cell ICR experiment. This discrepancy calls for a new measurement of the energy de-

[a] Geophysics Research Scholar.

[b] Air Force Office of Scientific Research, Bolling AFB, Washington, D.C., 20332.

 0021-9606/90/021117-09$03.00

pendence of the cross section for charge transfer between N_2^+ and H_2O.

In addition to the cross section measurements, time-of-flight measurements of the reaction products have been conducted in order to determine the kinetic energy release of the product ions. These measurements enable a qualitative assessment of the reaction dynamics involved in reactions (2a) and (2b).

II. EXPERIMENTAL

The apparatus used in this work is shown schematically in Fig. 1. It is an upgraded version of a tandem mass spectrometer described previously.[18] Ions are produced in either a dc discharge or an electron impact ion source. The discharge ion source (Colutron Research) is used when high ion beam intensities are needed as in the time-of-flight measurements. The electron impact source is used for the cross section measurements for which low ionization energies are desired to avoid metastable ion production. An ionization energy of 20 V is generally used. The low ionization energy does not circumvent vibrational excitation of the ions. The degree of vibrational excitation is monitored by measuring the charge transfer cross section of $N_2^+ + Ar$, for which the vibrational dependence is known.[19] We find that approximately 50% of the N_2^+ ions are vibrationally excited. The energy resolution of the primary ion beam is determined by the ion source conditions and is approximately 500 meV FWHM when using the discharge source and slightly less when using the electron impact ion source. The collision energy resolution however, is mainly governed by thermal broadening at the energies of interest in this work. The relatively low primary ion energy resolution consequently does not affect the accuracy of the present collision energy calibration.

The ions are accelerated to approximately 150 V and passed through a Wien velocity filter (Colutron Research) to produce a mass selected ion beam. The beam is decelerated in a first retardation lens to a minimum of 20 V before it is passed through a deflector electrode set, which is used to produce ion pulses for the time-of-flight experiments. The ions may be further decelerated in a second retardation lens between the deflector electrode and the collision chamber.

Water vapor is introduced into a 2.7 mm long collision chamber with gold-mesh covered apertures through which the ion beam is passed. The wire mesh prevents the penetration of the ion acceleration field into the collision chamber. The wire mesh also enhances the neutral density drop-off exterior to the collision chamber boundaries, allowing a more accurate definition of the effective interaction length. The exit aperture of 3.2 mm diameter is larger than the entrance aperture of 1.4 mm diameter to improve the collection efficiency. The neutral target pressure is measured with a capacitance manometer (MKS Baratron 390H). The pressure in the collision chamber is kept below 0.133 Pa (10^{-3} Torr) to ensure single collision conditions. A series of three collector grids, the first of which is hemispherically shaped, is then used to accelerate and focus the primary beam and the product ions onto the entrance aperture of an ELF quadrupole mass filter. The hemispherical grid potential is carefully adjusted to optimize both the primary and product ion beam signals. The ions are detected with a channel electron multiplier.

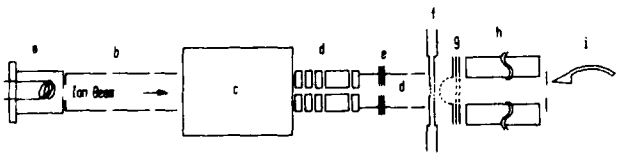

FIG. 1. Schematic of ion-neutral collision apparatus. The various elements are not drawn to scale. (a) Ion source (b) Acceleration lens. (c) Wien velocity filter. (d) Deceleration lenses. (e) Deflector electrode. (f) Collision chamber. (g) Acceleration and focusing grids. (h) Quadrupole mass filter. (i) Channel electron multiplier.

The primary ion energy is determined by ramping a retardation potential on one of the grids following the collision chamber. The derivative of the obtained retardation curve exhibits a minimum at which the ion beam energy is defined. The energies determined by this procedure are verified by measuring time-of-flight spectra of the primary beam. The ion times of flight are converted to ion energies using basic electrostatic equations. The time of flight and retardation measurements produce essentially the same energies. We estimate the uncertainty in the ion energy to be ± 0.3 eV.

The presence of metastable states[20,21] in the N_2^+ beam is checked by measuring the electron energy dependence of the cross sections when using the electron impact source. The cross sections are found to be independent of the electron energy at electron energies below 30 V.

When determining reaction cross sections, the collision chamber is biased at 80 to 100 V with respect to the quadrupole bias potential. No focusing is performed with the second deceleration lens in order to generate as parallel a primary beam as possible within the collision chamber, thus minimizing discrimination. The collector grid potentials are then adjusted to accept as wide a product scattering angle as possible. Ions scattered at very large angles in the laboratory frame as well as backward scattered ions do not exit the collision chamber and therefore are not detected. The method used to correct for this problem will be discussed below. Low-resolution mass spectra are recorded using an AT-compatible computer converted to a multichannel scaler. The resolution of the quadrupole mass filter is kept as low as possible in order to maintain a mass filter transmission which is independent of mass. The intensities of the primary and the secondary ion beams are obtained by integrating the peaks attributed to the respective masses. Since the small neutral density and effective path length cause no detectable attenuation of the primary beam intensity, the cross section σ can be determined from

$$\sigma = I_s/I_p nl, \tag{3}$$

where I_s is the secondary ion intensity, I_p is the primary ion intensity, n is the target gas density, and l is the effective interaction length.

The detection efficiency of channeltrons is known to be mass dependent.[22,23] The efficiency is reported to exhibit the most prominent mass discrimination at low masses (< 20 amu) and at low detector bias voltages. It is therefore possible that our measured cross sections for reaction (2a) are

slightly affected. This was checked by measuring cross sections at different bias voltages ranging from 1 to 2.5 kV. The cross sections are found to be independent of the detector bias voltage. We therefore conclude that the mass dependence of the detector efficiency is insignificant.

In order to determine the true integral cross section, the collection efficiency of the product ions must be ascertained. In hydrogen atom transfer reactions such as reaction (2b) there is typically very little momentum transfer and the angular distribution of the product ions in the laboratory frame is distinctly centered in the forward direction. In this case, the secondary ions are collected as efficiently as the primary ions. The cross section obtained is therefore equal to the integral cross section provided the true integral cross section is not significantly energy dependent within the energy width of the primary ion beam. We have measured the cross section of the hydrogen-atom transfer reaction

$$N_2^+ + D_2 \rightarrow N_2D^+ + D \qquad (4)$$

and compare our results to those obtained by Turner *et al.*[24] Shown in Fig. 2, our results are within 10% of those reported in Ref. 24. In this reaction, the main uncertainty lies in the effective path length l. The collision chamber path length was used for l to obtain the cross sections shown in Fig. 2. We estimate our measurements to be uncertain by $\pm$ 20%.

As mentioned above, in the case of reactions with large scattering angles in the laboratory frame, it is not possible in this experiment to collect the secondary ions as efficiently as the primary ions. If the product ion angular distribution is determined to be isotropic in the laboratory frame, the correct integral cross section can be obtained if the collection angle of the experiment is known. The collection efficiency of the present system has been calculated for thermal product ions by numerically integrating the collection angle throughout the interaction volume.[25] A collection efficiency of 18.0% is calculated. To test this value, the cross section of reaction (1) is measured and the raw data is corrected with respect to the collection efficiency before comparing our results to the known cross section.[15]

In order to measure the cross section of reaction (1), O^+ ions are generated by electron impact on CO_2.[26] Time-of-flight measurements performed in this laboratory show that the product H_2O^+ energy distributions are essentially thermal at center-of-mass energies ranging between 2 and 20 eV.[25] Hence, the calculated collection efficiency may be used to correct the raw cross sections. Our corrected data is compared to the measurements of Heninger *et al.*[15] in Fig. 3. The agreement is excellent. There is only a slight discrepancy at the lowest collision energy which may be due to a broader angular distribution of the products in the center-of-mass frame at this energy, resulting in a lower collection efficiency.

The time-of-flight technique used here is similar to previously reported techniques.[18,27] Both the collision chamber and the hemispherical grid are biased at a lower voltage of approximately 20 V to increase the flight time and therefore increase the time-of-flight resolution. At voltages below 15 V, the quadrupole mass filter seriously distorts the time-of-flight distributions. Primary ion pulse widths of 0.5 to 1.5 μs are obtained by pulsing the deflector electrode. A delayed pulse triggers a time-to-digital converter (20 ns resolution) for which the amplified and discriminated detector pulses provide the stop pulses. The time-of-flight spectra are recorded with the same computer used for the cross section measurements.

III. RESULTS

A. Charge exchange channel

The energy dependence of the cross section for reaction (2a) is shown in Fig. 4 for both H_2O and D_2O. The measured cross sections are listed in Table I. No difference is found between the two isotopically different reactions. A sample time-of-flight spectrum of the product ion H_2O^+ measured at a center-of-mass collision energy of 7.24 eV is

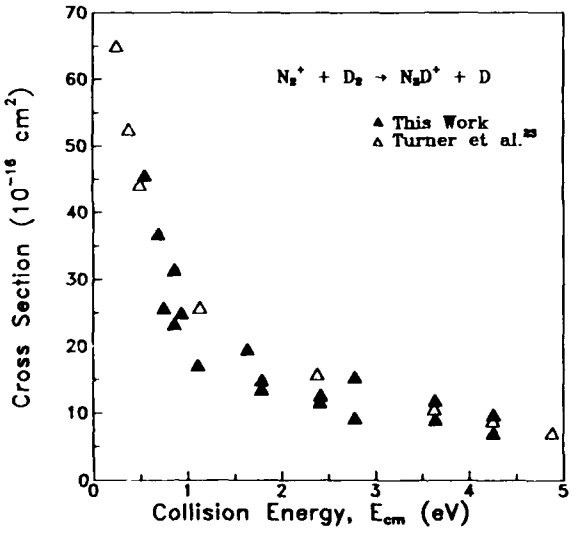

FIG. 2. Ion energy dependence of the cross section for the reaction $N_2^+ + D_2 \rightarrow N_2D^+ + D$. The data obtained in the present work is compared to the measurements of Turner *et al.* (Ref. 24).

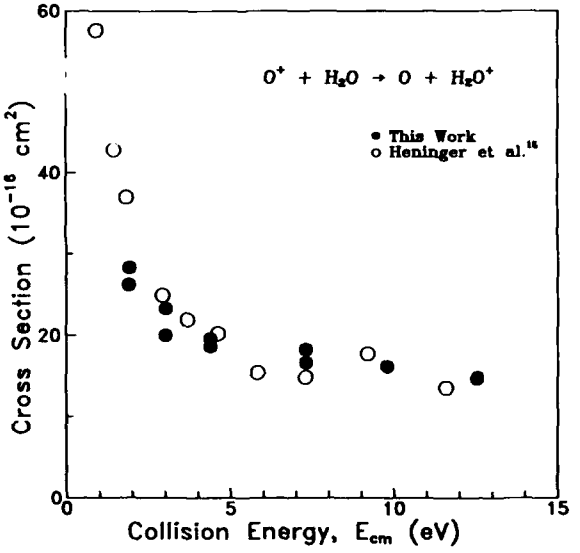

FIG. 3. Collision energy dependence of the charge exchange cross section for $O^+ + H_2O$ collisions. The data obtained in the present work has been corrected with respect to a collection efficiency of 18% and is compared to the measurements of Heninger *et al.* (Ref. 15).

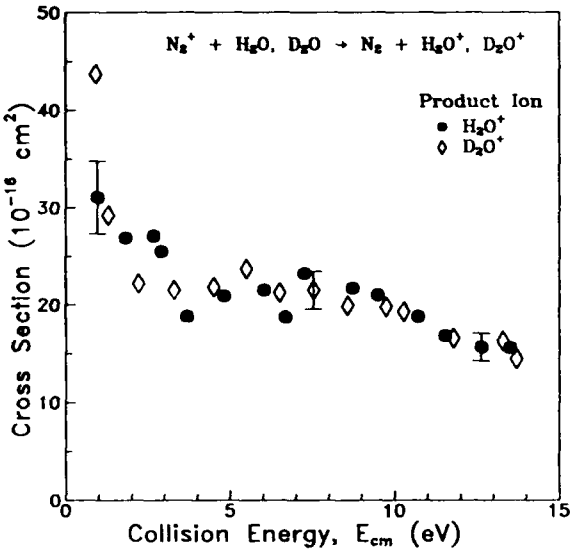

FIG. 4. Collision energy dependence of the charge exchange cross section for $N_2^+ + H_2O(D_2O)$ collisions. The data has been corrected with respect to a collection efficiency of 18% assuming an isotropic product distribution in the laboratory frame. The indicated errors are random errors, the systematic error is estimated to be approximately 30%.

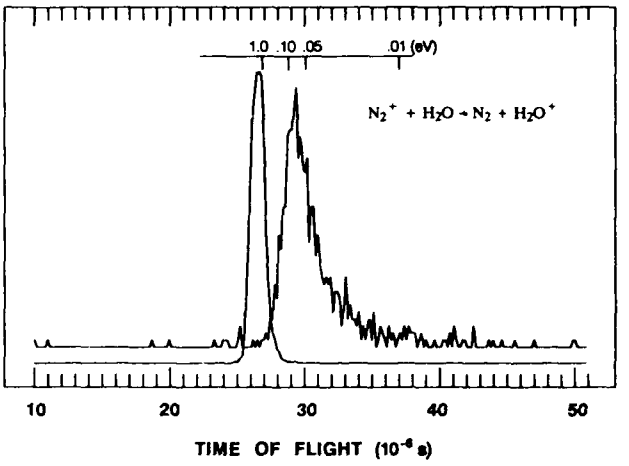

FIG. 5. Time-of-flight spectrum of H_2O^+ (upper curve) produced through charge exchange with N_2^+ at a collision energy of 7.24 eV (c.m.). The lower curve is the time-of-flight spectrum of the primary ion N_2^+. The inserted scale portrays the converted laboratory energies of H_2O^+ calculated assuming the product ions are produced in the collision chamber center and with a scattering angle of 0°.

shown in Fig. 5. The time-of-flight spectrum of the primary beam is also shown to demonstrate the time resolution of this particular measurement. The time resolution of approximately 0.5 μs is found to degrade at primary ion energies below 8 eV. The inserted scale represents the product laboratory ion kinetic energy calculated assuming the ions are formed in the center of the collision chamber. The time-of-flight spectra are very similar throughout the energy range investigated in this work. The calculated laboratory and center-of-mass kinetic energies of the H_2O^+ time-of-flight peak maxima are listed in Table II along with the corresponding center-of-mass collision energies. With the exception of the lowest collision energies, the H_2O^+ product distributions are found to be essentially thermal in the laboratory frame.

TABLE I. Measured cross sections for charge exchange in $N_2^+ + H_2O(D_2O)$ collisions. σ_{exp} is the experimentally obtained cross section and σ_{corr} is the cross section obtained when correction with respect to the collection efficiency of thermal ion products.

	$E_{c.m.}$ (eV)	σ_{exp} (Å^2)	σ_{corr} (Å^2)		$E_{c.m.}$ (eV)	σ_{exp} (Å^2)	σ_{corr} (Å^2)
H_2O	1.0	5.59	31.1	D_2O	0.9	7.86	43.7
	1.8	4.84	26.9		1.3	5.26	29.2
	2.7	4.88	27.1		2.2	3.99	22.2
	2.9	4.59	25.5		3.3	3.87	21.5
	3.7	3.38	18.8		4.5	3.92	21.8
	4.8	3.76	20.9		5.5	4.27	23.7
	6.0	3.87	21.5		6.5	3.82	21.2
	6.7	3.37	18.7		7.5	3.87	21.5
	7.3	4.18	23.2		8.6	3.58	19.9
	8.7	3.91	21.7		9.8	3.56	19.8
	9.5	3.78	21.0		10.3	3.47	19.3
	10.7	3.38	18.8		11.8	2.98	16.6
	11.5	3.03	16.8		13.3	2.93	16.3
	12.6	2.82	15.7		13.7	2.60	14.4
	13.5	2.81	15.6				

The product ion time-of-flight measurements for reaction (2a) are almost identical to those observed for reaction (1).[25] In the $O^+ + H_2O$ reaction, correcting the experimentally obtained cross sections for the calculated collection efficiency leads to charge transfer cross sections in excellent agreement with those obtained in a triple cell ICR experiment.[15] The same correction is therefore applied to the measured cross sections of reaction (2a). The values shown in Fig. 4 have been corrected with respect to the calculated collection efficiency of the product ion collection optics. Both the raw data and the corrected cross sections are listed in Table I.

The determined integral cross sections which we report are not in good agreement with the measurements of Turner and Rutherford[17] who reported a nearly constant cross section of approximately 50×10^{-16} cm^2 in the energy range investigated in this work. Since these authors also published data in the same paper on measurements of reaction (1) which was in poor agreement with the measurements of the

TABLE II. H_2O^+ (D_2O^+) laboratory energies E_{lab} obtained from the measured time-of-flight peak centers of charge transfer products in $N_2^+ + H_2O(D_2O)$ collisions

	$E_{c.m.}$ (eV)	E_{lab} (eV)		$E_{c.m.}$ (eV)	E_{lab} (eV)
H_2O	0.8	0.20 ± 0.09	D_2O	1.7	0.31 ± 0.22
	1.5	0.10 ± 0.05		2.7	0.27 ± 0.20
	3.3	0.24 ± 0.13		4.0	0.12 ± 0.09
	5.0	0.09 ± 0.05		5.9	0.10 ± 0.07
	5.5	0.05 ± 0.04		8.0	0.08 ± 0.05
	6.1	0.07 ± 0.05		10.3	0.08 ± 0.05
	7.2	0.08 ± 0.05		11.2	0.11 ± 0.07
	7.6	0.07 ± 0.06		12.0	0.06 ± 0.04
	7.6	0.10 ± 0.05		14.4	0.04 ± 0.02
	7.9	0.05 ± 0.04			
	10.5	0.07 ± 0.03			
	13.2	0.02 ± 0.01			

ICR experiment,[15] we conclude that our measurements are more reliable than the data from Ref. 17.

B. Atom pickup channel

The energy dependence of the measured cross sections of reaction (2b) is shown in Fig. 6 for both H_2O and D_2O. In the case of $N_2^+ + H_2O$ the ion product $m/e = 29$ signal includes contributions from the intense $m/e = 28$ signal and from $^{14}N^{15}N^+$ primary ions which are poorly discriminated in the Wien filter. The N_2H^+ was obtained by subtracting a normalized mass spectrum obtained with no target gas from the spectrum recorded with a target gas. The uncertainty of 30% is consequently somewhat higher for these measurements.

Contrary to the charge exchange branch, an isotope effect is clearly observed here. Sample time-of-flight spectra are displayed in Figs. 7 and 8, showing the N_2D^+ product from $N_2^+ + D_2O$ collisions at collision energies of 3.96 and 12.0 eV. A time-of-flight spectrum of N_2D^+ ions resulting from collisions between N_2^+ and D_2 [reaction (4)] at a collision energy of 2.41 eV is shown for comparison in Fig. 9. Time-of-flight spectra of N_2H^+ from the H_2O and H_2 reactions could not be recorded due to the low signal intensities when the mass filter resolution is adjusted to adequately separate the primary beam from the product ions.

All of the time-of-flight spectra show that the N_2D^+ product ions are generated with a large amount of forward energy. Consequently, the product ions are collected efficiently and the measured cross sections may be regarded as integral cross sections. The peak energies of the time-of-flight bands are listed in Table III. Also listed are the corresponding center-of-mass collision energies. A low velocity tail is observed in all of the N_2D^+ (from D_2O) spectra. The tail in the N_2D^+ (from D_2) spectra is less pronounced. The arrows in Figs. 7 and 8 indicate the times-of-flight corresponding to ions produced with no kinetic energy release in the center-of-mass frame. In that case, the laboratory velocity of the products is the center-of-mass velocity. The N_2D^+ time-of-flight bands resulting from $N_2^+ - D_2O$ collisions are also found to be slightly broader than the respective bands observed in the reaction with D_2.

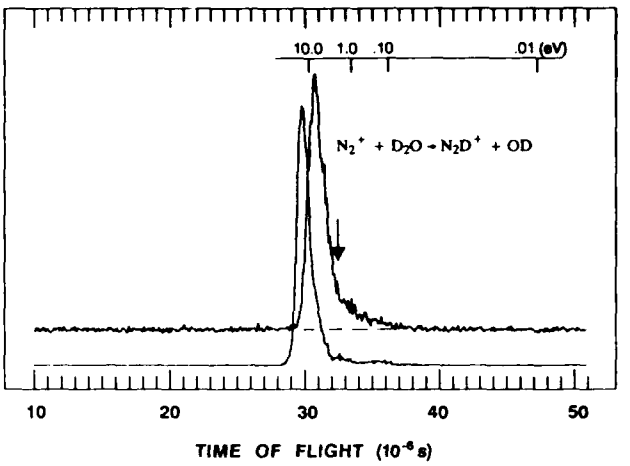

FIG. 7. Time-of-flight spectra of reactant ions (lower curve) and product ions (upper curve) of the reaction $N_2^+ + D_2O \rightarrow N_2D^+ + OD$ at a laboratory ion energy of 9.5 ± 0.5 eV (E_{cm} = 3.96 eV). The arrow indicates the time-of-flight corresponding to N_2D^+ produced at the respective center-of-mass velocity. The inserted scale portrays the converted laboratory energy of N_2D^+.

IV. DISCUSSION

A. Charge exchange channel

Figure 10 shows the relevant electronic energy levels of the charge exchange process [reaction (2a)]. The data is obtained from Rosenstock *et al.*,[28] Dixon *et al.*,[29] and Lew.[30] The charge exchange reaction has an exothermicity of 2.96 eV which is sufficient to populate the $A\,^2A_1$ state of H_2O^+. The $B\,^2B_2$ state becomes accessible at collision energies above 1.6 eV. Derai *et al.*[31] have observed A–X emission from thermal $Ar^+ - H_2O$ charge exchange collisions with an

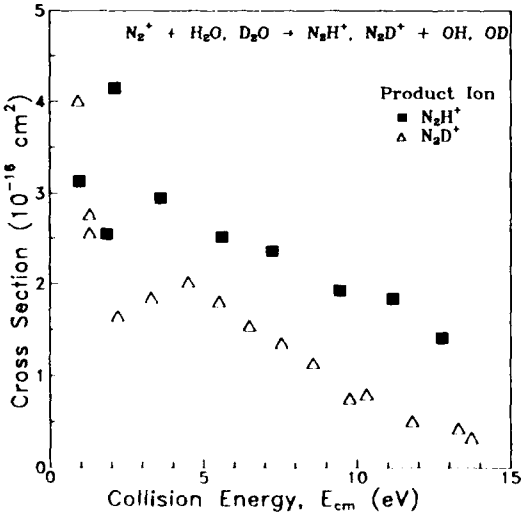

FIG. 6. Collision energy dependence of the reaction $N_2^+ + H_2O(D_2O) \rightarrow N_2H^+(N_2D^+) + OH(OD)$. The systematic errors are estimated to be approximately 20% for the deuterated and 30% for the hydrogenated reaction.

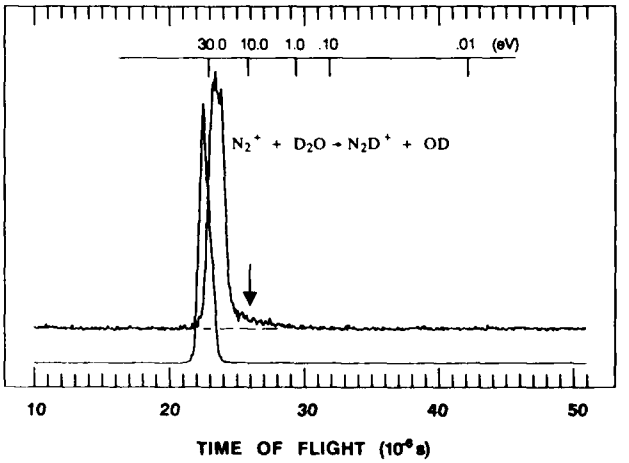

FIG. 8. Time-of-flight spectra of reactant ions (lower curve) and product ions (upper curve) of the reaction $N_2^+ + D_2O \rightarrow N_2D^+ + OD$ at a laboratory ion energy of 28.8 ± 0.5 eV (E_{cm} = 12.0 eV). The arrow indicates the time of flight corresponding to N_2D^+ produced at the center-of-mass velocity. The inserted scale portrays the converted laboratory energy of N_2D^+.

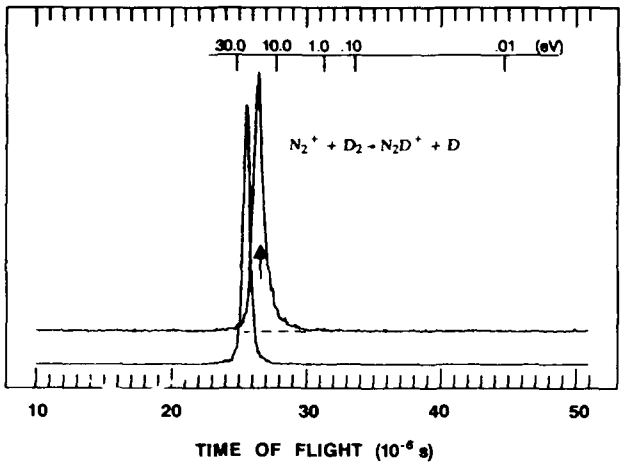

FIG. 9. Time-of-flight spectra of reactant ions (lower curve) and product ions (upper curve) obtained from the reaction $N_2^+ + D_2 \rightarrow N_2D^+ + D$ at an ion energy of 19.3 ± 0.5 eV ($E_{c.m.} = 2.41$ eV). The arrow indicates the time of flight corresponding to the center-of-mass velocity. The inserted scale shows the converted laboratory energy of N_2D^+.

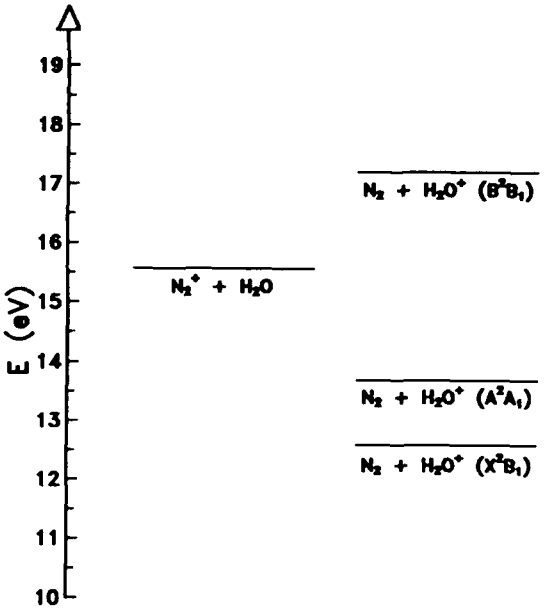

FIG. 10. Relevant electronic energy levels of the charge exchange process $N_2^+ + H_2O \rightarrow N_2 + H_2O^+$. The molecules are in the respective ground rovibronic states where not indicated.

exothermicity of 3.14 eV. Evidence for the formation of H_2O^+ $B\,^2B_2$ in the same reaction at energies above threshold has been presented by Glosik *et al.*[32] It is therefore conceivable that these excited states of H_2O^+ also become populated in the charge exchange reaction of $N_2^+ + H_2O(D_2O)$.

At collision energies above 4 eV, the H_2O^+ time-of-flight spectra show a single band at approximately thermal energies in the laboratory frame. The total kinetic energy release in the center-of-mass frame E_{kin} is then given by the center-of-mass collision energy $E_{c.m.}$. Including the thermal motion of the target this is[33]

$$E_{kin} = E_{c.m.} + (3/2)(m_1/M)kT = (m_2/M)E_{prim} + (3/2)(m_1/M)kT, \quad (5)$$

where m_1 is the primary ion mass, m_2 is the target neutral mass, M is the sum of the collision partner masses, and E_{prim} is the laboratory energy of the primary ions. The internal energy U of the products is then

$$U = E_{c.m.} - W - E_{kin} = -W - (3/2)(m_1/M)kT, \quad (6)$$

where W is the heat of reaction. Consequently, the internal energy of the collision products is approximately equal to the exothermicity of the charge transfer process.

TABLE III. N_2D^+ laboratory energies E_{sec} obtained from the measured ion product flight times of the $N_2^+ + D_2O$ atom pickup reaction. The primary (N_2^+) ion energy (E_{prim}) is also shown for comparison.

$E_{c.m.}$ (eV)	E_{prim} (eV)	E_{sec} (eV)
1.7	4.0	3.9
2.7	6.5	6.1
4.0	9.5	8.0
5.9	14.1	13.1
8.0	19.1	17.2
10.3	24.6	20.2
12.0	28.8	24.9
14.4	34.5	30.3

There is no evidence for higher laboratory-energy H_2O^+ ions which would be products with higher internal excitation or products scattered at larger angles. We therefore conclude that the charge transfer does not proceed via a long-lived complex at the collision energies above 4 eV. Furthermore, there is no evidence for the formation of H_2O^+ in the $B\,^2B_2$ state. Optical experiments need to be performed to determine the degree to which the H_2O^+ $A\,^2A_1$ state is populated.

The near-thermal laboratory energy distribution of the charge exchange product ions indicates that little to no momentum transfer occurs during the collision at energies above 4 eV. The charge exchange products are presumably formed in a small range of vibronically excited states. A similar behavior has been found in the most thoroughly studied ion–molecule charge exchange system at collision energies of interest in this work: $(Ar + N_2)^+$.[19,34–39] Govers *et al.*[19] studied experimentally the vibrational dependence of the N_2^+ (v) + Ar charge transfer cross section and could explain the significant vibrational dependence using diabatic vibronic potential curves and a Landau–Zener type model developed by Bauer *et al.*[40] The vibronic potentials used are given by the respective vibronic levels at infinite intermolecular distances and the long-range induced dipole and permanent quadrupole interactions. The model shows that in this particular reaction charge transfer occurs in most cases solely at the first crossing between the reactant and the product channel potentials encountered by the approaching reactants. Consequently only near-resonant transitions occur, resulting in a narrow product state distribution if a small number of reactant vibronic states are populated.

In a more sophisticated approach, Archirel and Levy[34] calculated *ab initio* potential curves of the $(Ar–N_2)^+$ system

including the repulsive part of the potentials as well as the electronic couplings. These authors found that the experimental results[19] are reproduced well when applying their calculated interactions to the charge transfer model of Demkov.[41]

The calculation of *ab initio* potential curves for the present system would present a formidable task. The use of diabatic potential curves as used in Ref. 19 is reasonable when considering that the relatively large charge transfer cross sections indicate that the transitions occur at large intermolecular distances where diabatic potentials are a good description of the interaction. The present system is more complicated, however, since a bimolecular reaction including a triatomic reactant is being examined. In addition to the problem of increased state density, the H_2O permanent dipole and the anisotropic polarizability and permanent quadrupole moment of N_2 render the interaction potential extremely anisotropic. The ion–dipole interaction will cause potential-curve crossings to occur at very large intermolecular separations R. Due to the weak electronic coupling at large R these crossings are not expected to foster efficient transitions. Consequently, more than one crossing may participate in the charge transfer process.

Dugan and co-workers[42–44] have solved numerically the equation of motion for a collision between an ion and a polar molecule. Their results indicate that even at thermal energies the dipole does not efficiently lock into the direction of the ion. This has been confirmed by similar calculations and expeiments by Su and Bowers.[45,46] The potentials at all possible orientations of the reactants must therefore be considered. Furthermore, the large degree of anisotropy in the interaction potential may lead to large degrees of rotational excitation which is not treated in the above model. A detailed discussion of the relevant long-range interaction potentials is not within the scope of this work and will be treated elsewhere.[47]

At energies below 3 eV, the cross sections increase rapidly with decreasing energy, indicating an increasing importance of the attractive part of the potential. The measured time-of-flight peaks, although subject to larger error bars, clearly show the product ion to be at higher laboratory velocities. This is due to either higher internal excitation of the reaction products or scattering at larger angles in the center-of-mass frame. The experiment presently is incapable of discerning between these two possibilities. These collision energies may be regarded as representing an intermediate range between a direct mechanism and one involving a long-lived complex where the long-range ion-permanent dipole and long-range ion-induced dipole interaction govern the outcome of the collision. In addition, adiabatic properties become more important at lower energies, significantly altering the dynamics.

B. Atom pickup channel

The similarity between the product ion time-of-flight spectra of reaction (2b) and (5) indicates that both reactions proceed via related mechanisms. Reaction (4) has been described as progressing via a spectator stripping mechanism.[48–53] According to this simple model the reaction effectively occurs between the transferred atom and the reactant ion while the residual neutral fragment is a "spectator" of the reaction. The product ion is then produced with a velocity corresponding to the center of mass of the atom and the reactant ion while the neutral spectator fragment recoils at the velocity of the neutral reactant. If the target is assumed to be stationary in the laboratory frame, the laboratory velocity of the product ion is given by

$$v_3 = [m_1/(m_1 + m_T)] \cdot v_1, \tag{7}$$

where v_1 is the reactant ion velocity, m_1 the reactant ion mass, and m_T the mass of the transferred atom. The laboratory energy of the product ion E_{sec} is then given by

$$E_{sec} = [m_1/(m_1 + m_T)] \cdot E_{prim}. \tag{8}$$

In the reactions of N_2^+ with H_2O and D_2O this yields a ratio E_{sec}/E_{prim} of 0.966 and 0.933, respectively.

The laboratory product ion energy of the deuterium pickup channel is plotted in Fig. 11 versus the laboratory primary ion energy. The dashed line indicates the secondary ion energy expected from the stripping model. The determined secondary ion energies converted from the measured flight times agree reasonably well with predicted values. The measured product energies are slightly below the values predicted by the model.

In the case of $N_2^+ + H_2(D_2)$ collisions, it has been found that the product ion velocities exceed the spectator stripping predictions at low ion energies and gradually approach them at higher ion energies.[48,51] A possible explanation for the behavior in reaction (2b) may be found in the stronger attractive short range chemical (bonding) interaction in the case of the H_2O target. This interaction may cause transfer of momentum to the spectator, resulting in a lower translational energy of the product ion. Higher resolution time-of-flight measurements are needed to clearly assess the situation.

The significant isotope effect is also consistent with the spectator stripping model. According to this mechanism, there should be no isotope effect at relative energies E_r based

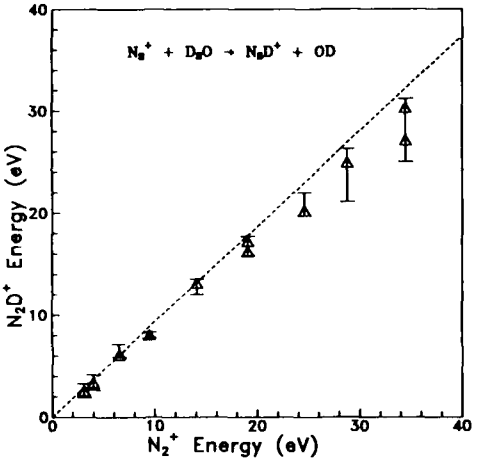

FIG. 11. Ion energy dependence of the laboratory energy of the N_2D^+ products formed by atom-pickup reactions of N_2^+ and D_2O. The dashed line shows the secondary ion energy predicted with the spectator stripping mechanism.

on the stripping model:

$$E_r = [m_I/(m_1 + m_I)] \cdot E_{\text{prim}}. \quad (9)$$

If the cross sections in Fig. 6 are plotted versus E_r, it is seen that the two isotopic cross sections essentially become equal.

The N_2D^+ spectra of reaction (2b) are found to be slightly broader than those observed in reaction (4). The broadening with respect to the primary beam half width is likely to be due to thermal broadening effects. The effects of the thermal motion of the target molecules on the collision energy distribution and the product kinetic energy distribution has been discussed by Chantry[53] and Gerlich.[54] In order to accurately evaluate the thermal broadening involved in the N_2D^+ time-of-flight peaks, the angular dependence of the differential cross section needs to be known. In the present experiment, isotropic scattering in the center-of-mass frame would result in a maximum time-of-flight width. The broadening observed in reaction (2b) may therefore be an indication that scattering at large angles is more important in reaction (2b) than in reaction (4).

A low velocity tail is present in the N_2D^+ (from D_2O) time-of-flight spectra which is not as prominent in the N_2D^+ (from D_2) spectra. The tail occurs at forward velocities which are smaller than the center-of-mass velocity indicated with the arrows in Figs. 7 and 8. It is therefore not likely that the tail ions originate from the collisions where most of the excess energy is partitioned into internal excitation. The band tail must therefore be due to ions scattered at large angles. Gentry *et al.*[49] detected small amounts of large-angle scattering with preference to products scattered at 180° c.m. in reaction (4). For this reaction the time-of-flight resolution of the present experiment is not sufficient to distinguish these ions as seen from the position of the arrow indicating the center-of-mass velocity in Fig. 9. In reaction (2b), however, the center-of-mass velocity is significantly smaller than the primary ion laboratory velocity vector so that the large-angle scattered ions can be resolved. The time-of-flight spectra do not indicate a preference for scattering at 180°. The large-angle scattering is presumably due to collisions with small impact parameters.

C. Relevance to spacecraft environment

As stated in the introduction, these measurements were carried out as part of a program aimed at understanding the dynamics of the plasma/neutral environment of large space structures, such as the space shuttle. For that purpose cross sections for ion-neutral reactions at suprathermal energies as well as information about the partitioning of the collision energy among the various modes of internal excitation and kinetic energy of the collision products are needed.

A spacecraft orbital velocity of 7.7 km s^{-1} corresponds to center-of-mass collision energies of 2.6 and 3.4 eV for reactions (1) and (2), respectively. The fact that we observe primarily thermal ions (lab frame) from reactions (1) and (2a) at these energies suggests that in the case of a high pressure local environment, the relevant cross sections for secondary reactions are those of thermal ions, as has indeed been suggested.[6,7] A more detailed analysis of the implications of reactions (1) and (2) on the shuttle environment will be treated elsewhere.[55]

ACKNOWLEDGMENTS

The authors wish to thank D. Gerlich, R. Lishawa, and A. Viggiano for helpful comments.

[1] J. C. Light, J. Chem. Phys. **40**, 3221 (1964).
[2] P. Pechukas and J. C. Light, J. Chem. Phys. **42**, 3281 (1965).
[3] J. C. Light and J. Lin, J. Chem. Phys. **43**, 3209 (1965).
[4] For an extensive experimental review see *Techniques for the Study of Ion–Molecule Reactions*, edited by J. M. Farrar and W. H. Saunders, Jr., (Wiley, New York, 1988).
[5] E. Teloy and D. Gerlich, Chem. Phys. **4**, 417 (1974).
[6] R. S. Narcisi, E. Trzcinski, G. Federico, L. Wlodyka, and D. Delorey, AIAA-83-2659, 183 (1983).
[7] J. M. Grebowsky, M. W. Pharo III, H. A. Taylor, Jr., and I. J. Eberstein, Planet. Space. Sci. **35**, 501 (1987).
[8] *Handbook of Geophysics and the Space Environment*, edited by A. S. Jursa, ADA 167000 (1985).
[9] D. E. Hunton and J. M. Calo, Planet. Space Sci. **33**, 945 (1985).
[10] E. Murad, Planet. Space Sci. **33**, 421 (1985).
[11] D. E. Hastings, N. A. Gatsonis, and T. Mogstad, J. Geophys. Res. **93**, 1961 (1988).
[12] G. E. Caledonia, J. C. Person, and D. E. Hastings, J. Geophys. Res. **92**, 273 (1987).
[13] J. B. Elgin, M. M. Perviaz, D. C. Cooke, M. Tautz, and E. Murad, J. Geophys. Res. (submitted).
[14] E. Murad and S. T. F. Lai, Chem. Phys. Lett. **126**, 427 (1986).
[15] M. Heninger, S. Fenistein, G. Mauclaire, R. Marx, and E. Murad, J. Geophys. Res. **16**, 139 (1989).
[16] C. J. Howard, H. W. Rundle, and F. Kaufman, J. Chem. Phys. **53**, 3745 (1970).
[17] B. R. Turner and J. A. Rutherford, J. Geophys. Res. **73**, 6751 (1968).
[18] W. B. Maier and E. Murad, J. Chem. Phys. **55**, 2307 (1971).
[19] T. R. Govers, P. M. Guyon, T. Baer, K. Cole, H. Fröhlich, and M. Lavollee, Chem. Phys. **87**, 373 (1984).
[20] A. Lofthus and P. H. Krupenie, J. Chem. Phys. Ref. Data **6**, 113 (1977).
[21] A. Anderson and E. W. Thulstrup, J. Phys. B **6**, L211–L213 (1973).
[22] C. A. Burrous, A. J. Lieber, and V. T. Zaviantseff, Rev. Sci. Instrum. **38**, 1477 (1967).
[23] W. E. Potter and K. Mauersberger, Rev. Sci. Instrum. **43**, 1327 (1972).
[24] B. R. Turner, M. A. Fineman, and R. F. Stebbings, J. Chem. Phys. **42**, 4088 (1965).
[25] J. A. Gardner, R. A. Dressler, R. H. Salter, and E. Murad, Geophys. Lab. Tech. Rep. (submitted).
[26] E. Murad, J. Chem. Phys. **58**, 4374 (1973).
[27] J. F. Paulson, F. Dale, and S. A. Studniarz, Int. J. Mass Spectrom. Ion Phys. **5**, 113 (1970).
[28] H. M. Rosenstock, K. Draxl, B. W. Steiner, and J. T. Herron, J. Chem. Phys. Ref. Data **6**, 1 (1977).
[29] R. N. Dixon, G. Duxbury, J. W. Rabalais, and L. Åsbrink, Mol. Phys. **31**, 423 (1976).
[30] H. Lew, Can. J. Phys. **54**, 2028 (1976).
[31] R. Derai, S. Fenistein, M. Gerard-Ain, T. R. Govers, R. Marx, G. Mauclaire, C. Z. Profous, and C. Sorisseau, Chem. Phys. **44**, 65 (1979).
[32] J. Glosik, B. Friedrich, and Z. Herman, Chem. Phys. **60**, 369 (1981).
[33] P. J. Chantry, J. Chem. Phys. **55**, 2746 (1971).
[34] P. Archirel and B. Levy, Chem. Phys. **106**, 51 (1986).
[35] M. R. Spalburg, J. Los, and E. A. Gislason, Chem. Phys. **94**, 327 (1985).
[36] M. R. Spalburg and E. A. Gislason, Chem. Phys. **94**, 339 (1985).
[37] E. A. Gislason and G. Parlant, Comments At. Mol. Phys. **19**, 157 (1987).
[38] B. Friedrich, W. Trafton, A. Rockwood, S. Howard, and J. H. Futrell, J. Chem. Phys. **80**, 2537 (1984).
[39] A. L. Rockwood, S. L. Howard, W. H. Du, P. Tosi, W. Lindinger, and J. H. Futrell, Chem. Phys. Lett. **144**, 486 (1985).
[40] E. Bauer, E. R. Fisher, and F. R. Gilmore, J. Chem. Phys. **51**, 4173 (1969).
[41] Y. N. Demkov, Sov. Phys. JETP **18**, 138 (1964).
[42] J. V. Dugan and J. L. Magee, NASA Report No. TN-D-3229, February, 1966.
[43] J. V. Dugan and J. L. Magee, J. Chem. Phys. **47**, 3101 (1967).
[44] J. V. Dugan, J. H. Price, and J. L. Magee, Chem. Phys. Lett. **3**, 323 (1969).

[45]T. S[illegible] M. T. Bowers, Int. J. Mass Spectrom. Ion Phys. **12**, 347 (1973).
[46]T. Su and M. T. Bowers, J. Chem. Phys. **58**, 3027 (1973).
[47]R. Dressler and J. A. Gardner (in preparation).
[48]Z. Herman, J. Kerstetter, T. Rose, and R. Wolfgang, Discuss. Faraday Soc. **44**, 123 (1967).
[49]W. R. Gentry, E. A. Gislason, Y. T. Lee, B. H. Mahan, and C. W. Tsao, Discuss. Faraday Soc. **44**, 137.
[50]A. Henglein, in *Proceedings of the International School of Physics "Enrico Fermi", C. XLIV, Mol. Beams and Kinetics*, edited by Ch. Schlier (Academic, New York, 1970).
[51]K. Lacmann and A. Henglein, Ber. Bunsenges. Phys. Chem. **69**, 292 (1965).
[52]A. Ding, K. Lacmann, and A. Henglein, Ber. Berl. Buns. Ges. **71**, 596 (1967).
[53]A. Henglein, Adv. Mass Spectrom. **3**, 331 (1966).
[54]D. Gerlich, J. Chem. Phys. **90**, 127 (1989).
[55]E. Murad, R. A. Dressler, and J. A. Gardner (in preparation).